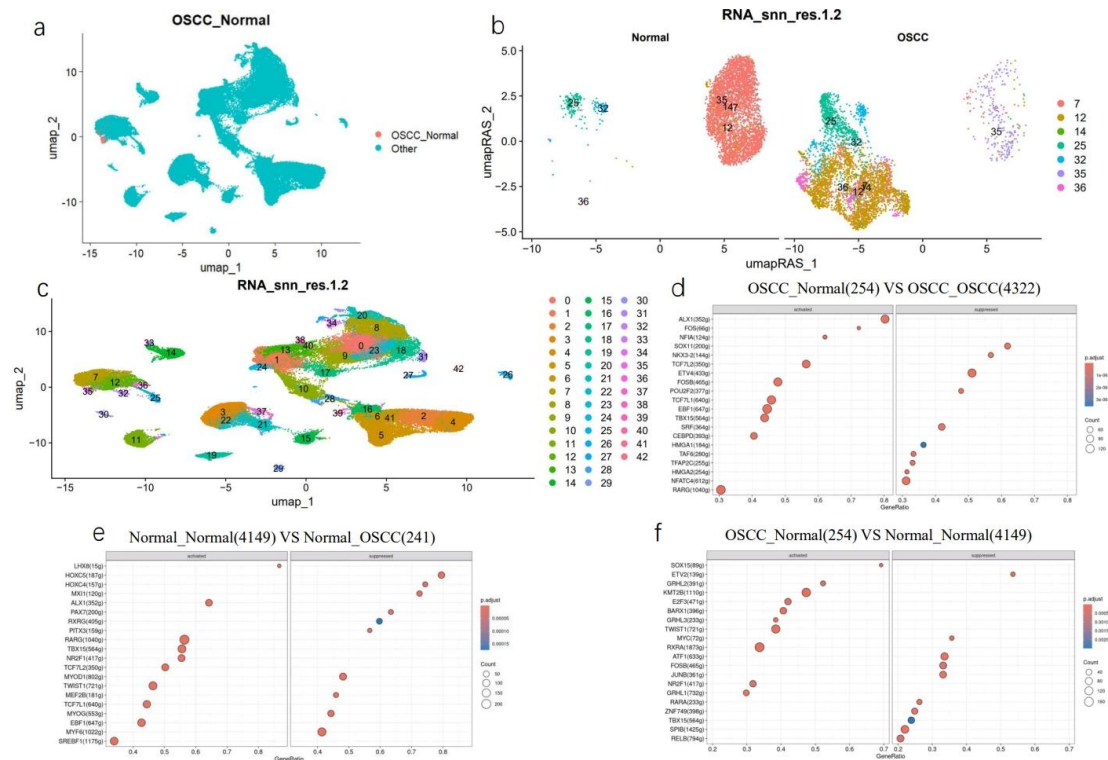


Supplementary Materials

Multi-Omics Analysis Reveals that Tumor Epithelial Cells in Oral Squamous Cell Carcinoma Regulate Oxidative Stress Defense to Counteract Resistance from Cancer-Associated Fibroblasts and Promote Tumor Progression

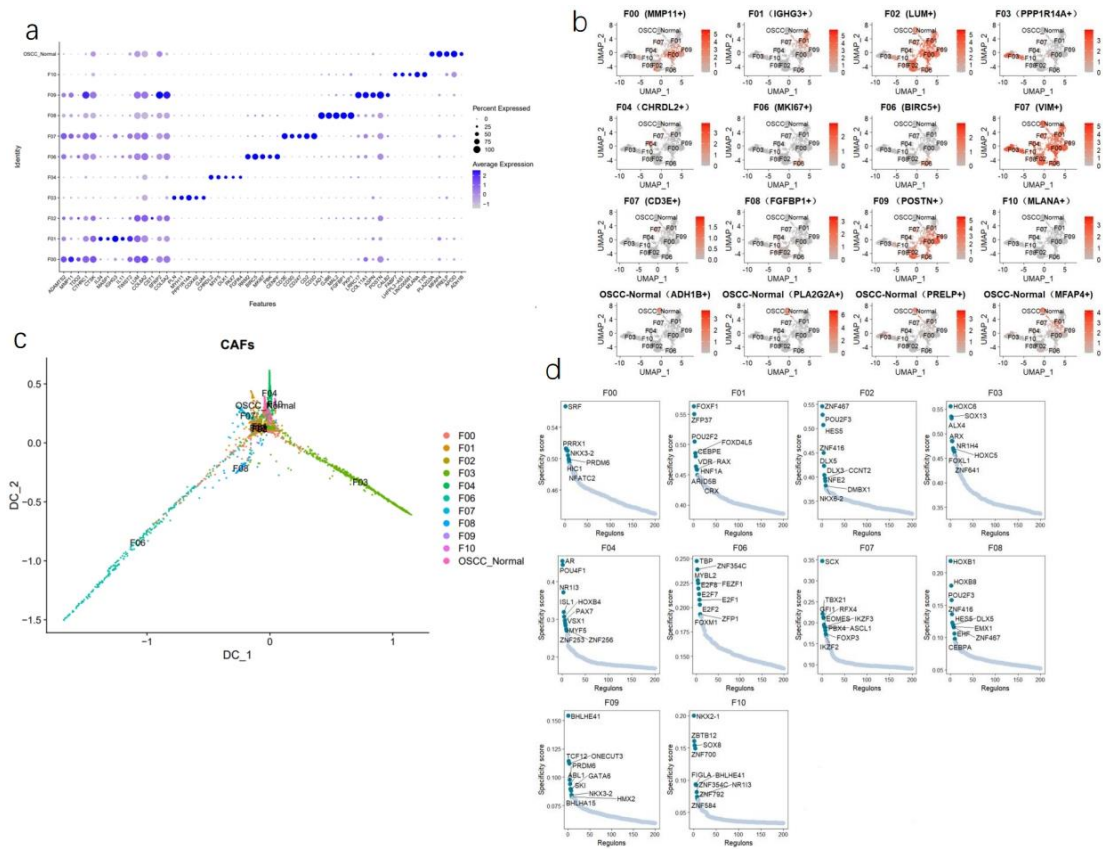
Hongrang Zhang, Yemei Qian, Yang Zhang, Xue Zhou, Shiyong Shen, Jingyi Li, Zheyi Sun, Weihong Wang



Supplementary Figure 1

Differential Transcription Factor Activity and Cell Population Distribution Between OSCC and Normal Cells.

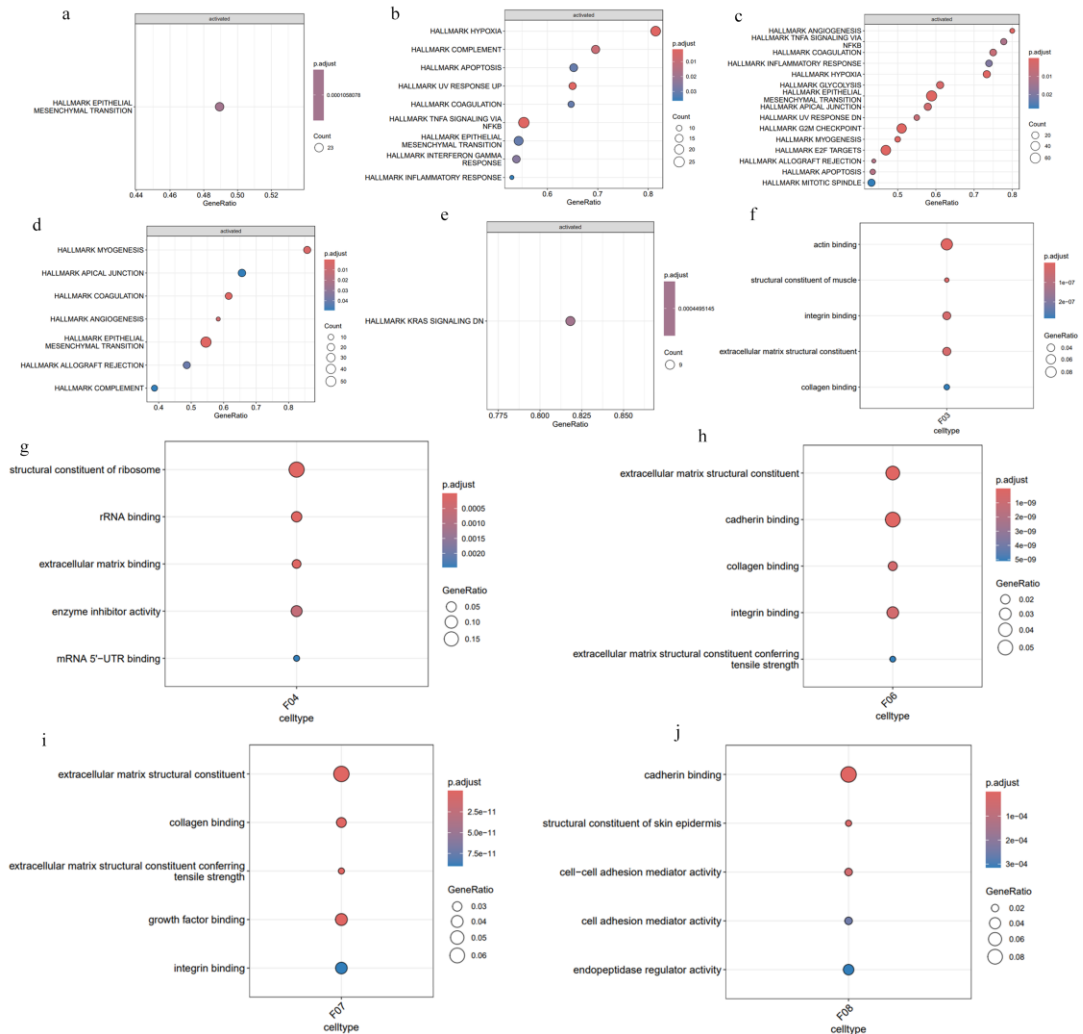
a. UMAP visualization highlighting the location of OSCC_Normal in the entire atlas, with red highlighting marking the OSCC_Normal cell cluster. b. Fibroblast clustering state under UMAP_RAS1 dimensionality reduction at a resolution of 1.2, with the C35 cluster being close to OSCC_Normal. c. UMAP displaying the entire atlas of cell populations at a resolution of 1.2, with different colors representing different cell populations. d. Comparison of transcription factor activity differences between OSCC_Normal and OSCC_OSCC in fibroblasts. The size of the dots represents gene expression levels, and the color intensity indicates the statistical significance of expression differences, with the number of cells in parentheses. e. Transcription factor activity differences between Normal_Normal and Normal_OSCC cells. f. Comparison of transcription factor activity between OSCC_Normal and Normal_Normal fibroblasts, emphasizing gene regulatory features similar to normal cells in the CAFs cell population.



Supplementary Figure 2.

Analysis of Gene Expression and Trajectories in CAF Subgroups

a. Dot plot of gene expression showing the top 5 gene expression levels and expression percentages of each CAF subgroup (F00 to F10 and OSCC_Normal). b. UMAP visualization highlighting key marker genes of specific subgroups. c. Single-cell trajectory analysis plot showing the branching paths originating from the OSCC-Normal cell cluster, pointing to the five main branches (F03, F04, F06, F07, F08), revealing the dynamic evolution of CAF state transitions and fibroblast functions. d. Specific transcriptional regulators of CAF subgroups.

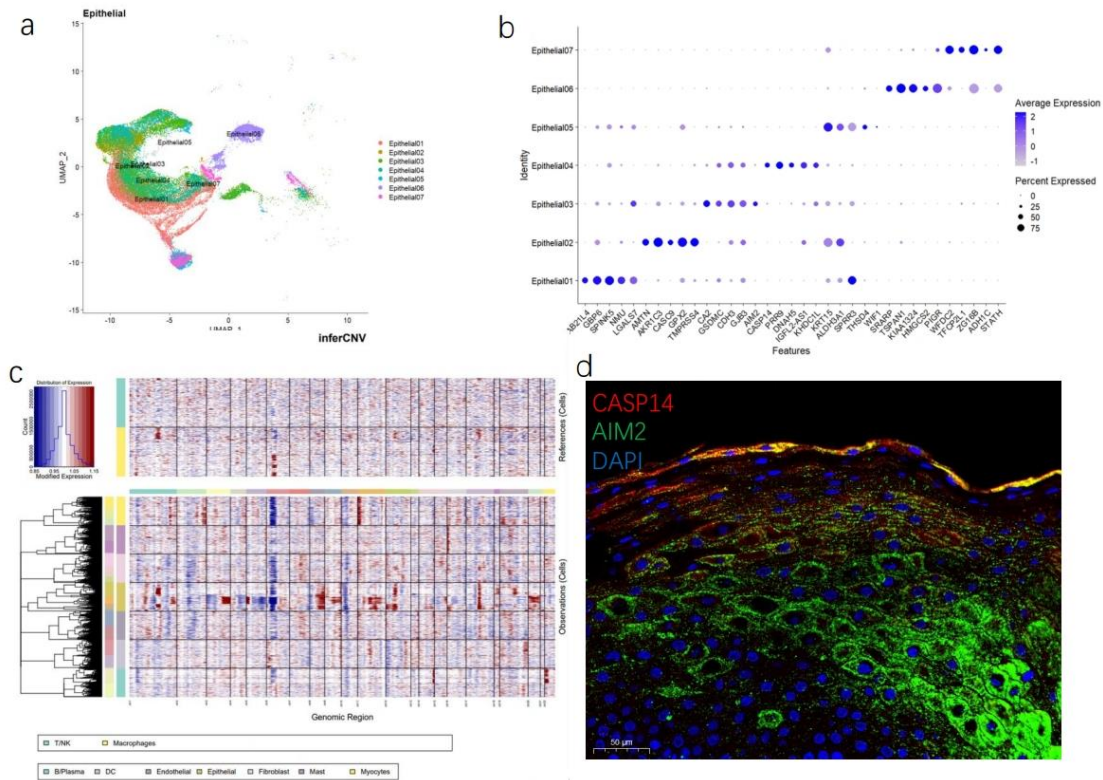


Supplementary Figure 3.

Functional Activation and Gene Expression Characteristics Analysis of CAF Subgroups in OSCC

a. The F03 subgroup significantly activates the epithelial-mesenchymal transition (EMT) process in OSCC, with a schematic showing the activation state and gene proportions of related gene sets. b. Functional characteristics of the F04 subgroup, primarily showing significant activation of the hypoxia response, complement, and NF- κ B mediated TNF- α signaling pathways. c. The F06 subgroup activates multiple key biological processes in OSCC, including angiogenesis, inflammatory response, hypoxia, and EMT, reflecting its potential role in promoting tumor progression in the tumor microenvironment. d. The F07 subgroup shows significant activation of myogenesis, blood coagulation, and EMT processes, suggesting these cells may play an important role in structural remodeling and cell migration in the tumor microenvironment. e. Unique functional state of the F08 subgroup, showing downregulation of the KRAS signaling pathway, which may affect the proliferation and survival ability of this subgroup. f. GO analysis results of the F03 subgroup, highlighting functions in ECM composition and actin binding. g. Gene function analysis of the F04 subgroup, revealing significant activity in ribosomal structure components and rRNA binding. h. GO functions of the F06 subgroup indicate significant activities in ECM structural components, cadherin

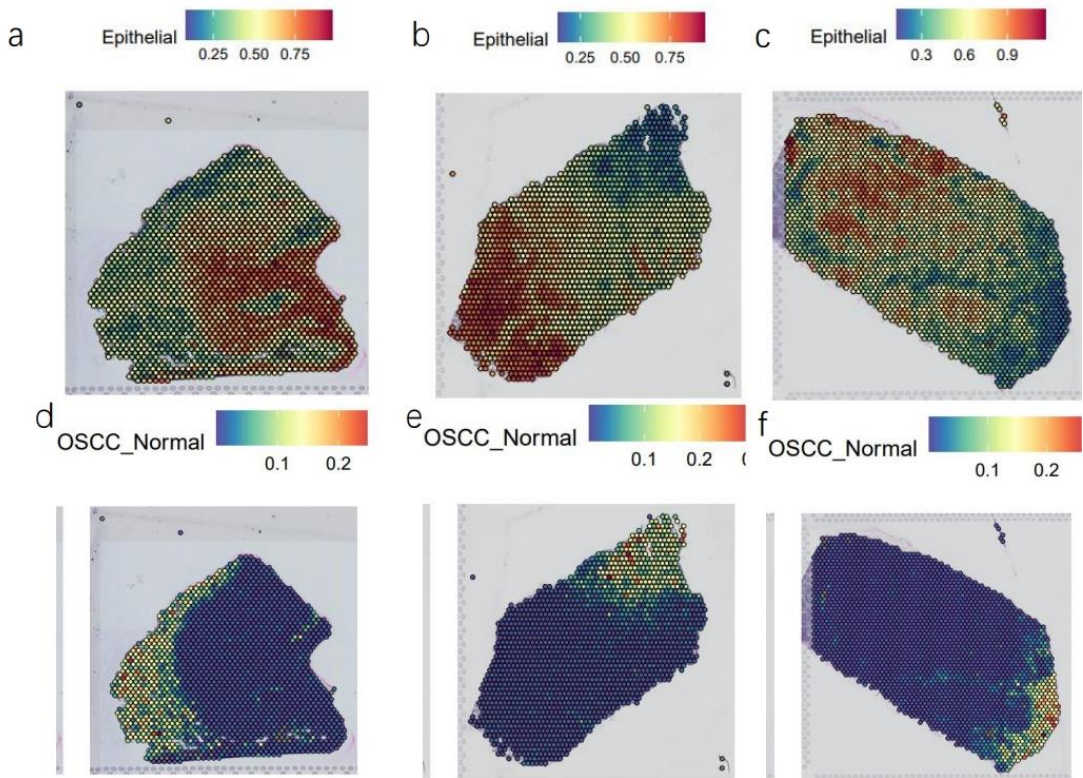
binding, collagen binding, and integrin binding, reflecting its key role in cell adhesion and matrix remodeling. i. Functional analysis of the F07 subgroup shows activity in ECM composition, collagen binding, and growth factor binding, possibly related to its role in cell migration and signal regulation. j. Gene function analysis of the F08 subgroup highlights specific activities in cell adhesion and skin epidermis structural components, possibly related to cell-cell interactions and maintaining structural integrity.



Supplementary Figure 4

Identification and Validation of Epithelial Cell Subpopulations.

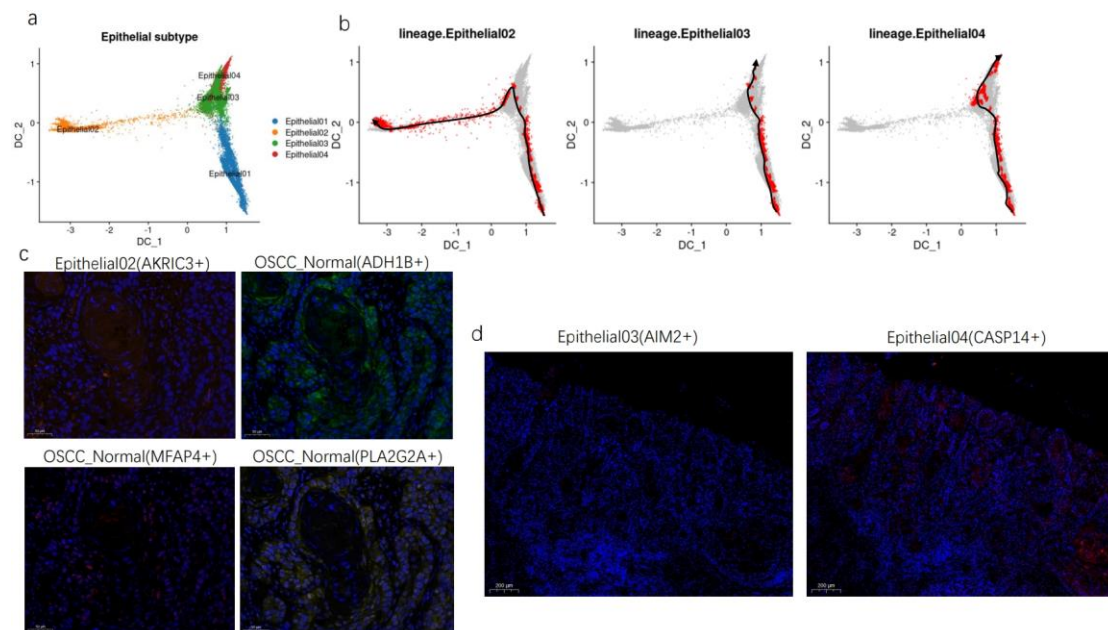
a. UMAP dimensionality reduction shows epithelial cells under the GRN algorithm, with cell clusters mixed across the UMAP. b. A dot plot illustrates the expression levels and expression percentages of the top 5 genes in each epithelial cell subgroup. c. A heatmap displays the CNV variations of cell clusters analyzed from the reference perspective of normal cells (macrophages and T/NK cells). Red indicates CNV amplification, and blue indicates CNV deletion. The X-axis represents chromosome numbers, and the Y-axis represents the cell clusters included in the analysis. d. Fluorescence in situ hybridization validates the expression of specific epithelial cell markers in tissues. The image shows cells marked as Epithelial 04 (CASP14+) and Epithelial 03 (AIM2+), with nuclei stained by DAPI.



Supplementary Figure 5

Spatial Transcriptomics Analysis of Epithelial and OSCC_Normal Cell Cluster Distribution in OSCC Samples.

a-f. The spatial transcriptomics display the distribution of epithelial cell clusters and OSCC_Normal cell clusters in OSCC samples. The top of each panel shows the expression intensity for each cell cluster, with darker colors indicating higher intensity.

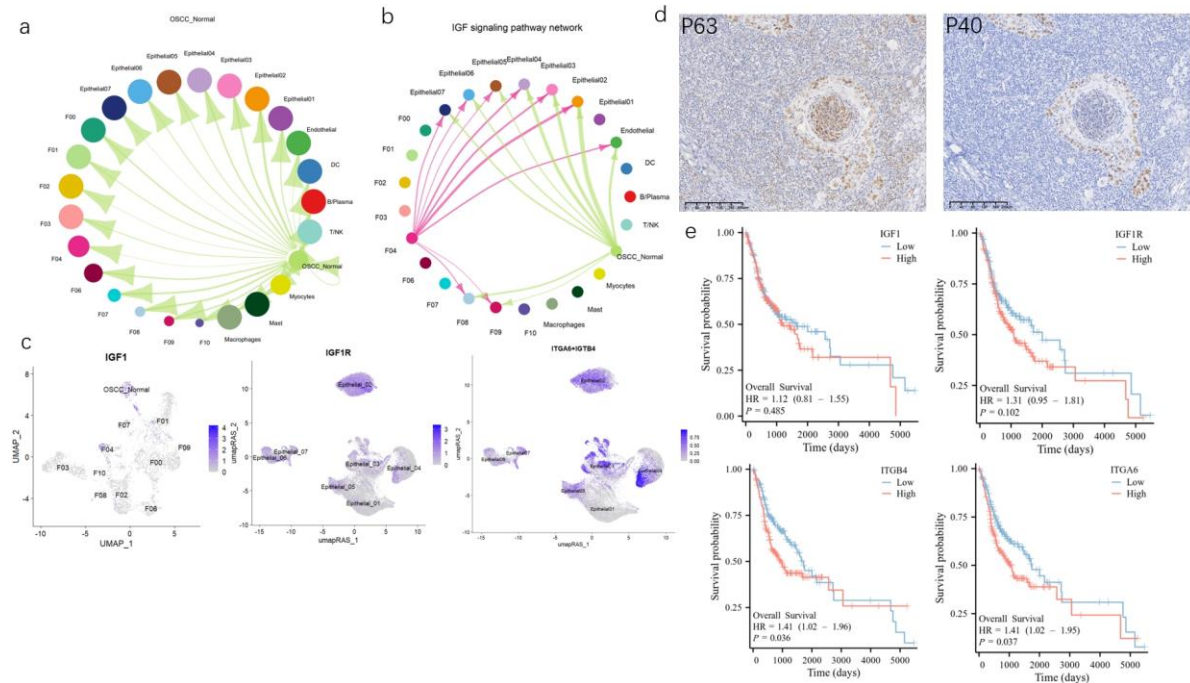


Supplementary Figure 6

Single-Cell Trajectory Analysis and Immunofluorescence Staining of Epithelial Subsets

in OSCC.

a, b. Single-cell trajectory analysis charts showing branching paths from epithelial subset 01, leading to three main branches (epithelial subsets 02, 03, 04), revealing the potential progression of malignant epithelial cells. c. Immunofluorescence staining of characteristic markers for epithelial subset 02 and OSCC_Normal in OSCC. d. Immunofluorescence staining of characteristic markers for epithelial subsets 03 and 04 at the tumor invasion front. e. Immunofluorescence staining of characteristic markers for epithelial subsets 03 and 04 at the tumor invasion front.



Supplementary Figure 7

Interaction Strength and IGF Signaling Pathway Network in OSCC_Normal and OSCC Cell Clusters.

a. The communication intensity between cell populations in OSCC_Normal and OSCC is displayed, with thicker lines representing a greater number of interactions and stronger interaction weight/intensity between the two cell types. b. A detailed representation of the insulin-like growth factor (IGF) signaling network is provided, where thicker lines indicate a greater number of interactions and stronger interaction weight/intensity between the two cell types. c. The expression intensity of the IGF1 ligand and its receptors IGF1R and ITGA6+ITGB4 within cell subpopulations is visualized using UMAP-RAS. d. Immunohistochemical staining of OSCC tissue is shown, with P63 on the left and P40 on the right. e. The prognostic outcomes for OSCC cohort patients regarding IGF1, IGF1R, ITGB4, and ITGA6 are presented, with red representing patients with high expression of these genes and blue indicating low expression. The vertical axis represents survival probability, while the horizontal axis represents survival time.